Concise Report

thiopeptides, biosynthesis, piperidine, $F_{420}H_2$-dependent reductase, $TppX_4$

CJC Chinese Journal of Chemistry 中国化学 An International Journal

Biosynthesis of the Central Piperidine Nitrogen Heterocycle in Series *a* Thiopeptides

Jingyu Liu,[a,‡] Zhi Lin,[a,c,‡] Hua Chen,[a] Heng Guo,[a] Jiang Tao,[b] and Wen Liu*[,a,d]

[a] *State Key Laboratory of Bioorganic and Natural Products Chemistry, Center for Excellence on Molecular Synthesis, Shanghai Institute of Organic Chemistry, University of Chinese Academy of Sciences, 345 Lingling Road, Shanghai 200032, China*
[b] *Department of General Dentistry, Ninth People's Hospital, Shanghai Jiao Tong University School of Medicine, Shanghai Key Laboratory of Stomatology, Shanghai 200011, China*
[c] *State Key Laboratory of Microbial Metabolism, School of Life Science & Biotechnology, Shanghai Jiao Tong University, 800 Dongchuan Road, Shanghai 200240, China*
[d] *Huzhou Center of Bio-Synthetic Innovation, 1366 Hongfeng Road, Huzhou, Zhejiang 313000, China*

Cite this paper: *Chin. J. Chem.* **2019**, *37*, 35—41. **DOI: 10.1002/cjoc.201800497**

Summary of main observation and conclusion Thiopeptides, arising from complex posttranslational modifications of a genetically encoded precursor peptide, are of great interest due to their structural complexity and important biological activities. All of these antibiotics share a macrocyclic peptidyl core that contains a central, six-membered nitrogen heterocycle and are classified into five series *a*—*e* based on the oxidation state of the central nitrogenous ring. Here, we report that the biosynthesis of the central piperidine heterocycle of series *a* thiopeptides relies on the activity of homologues of an $F_{420}H_2$-dependent reductase $TppX_4$ by exploiting and characterizing the piperidine-containing thiopeptin biosynthetic gene *(tpp)* cluster in *Streptomyces tateyamensis*. *In vitro* reconstruction of $TppX_4$ activity demonstrated that the piperidine heterocycle of thiopeptins was transformed from a dehydropiperidine heterocycle, and $TppX_4$ tolerated the changes in the C-termini and macrocyclic peptidyl core of substrate and also tolerated dehyropiperidine-containing monocyclic or bicyclic thiopeptides. The identification of $TppX_4$ and its substrate tolerance enriches the biosynthetic toolbox for development of additional thiopeptide analogs for clinical drug screening.

Background and Originality Content

Thiopeptide antibiotics are a class of sulfur-rich, ribosomally synthesized and post-translationally modified peptide (RiPP) natural products. These antibiotics possess a wide variety of biological activities, *e.g.*, anti-infection, antitumor and immunosuppression and are beneficial to humans largely because of their highly functionalized unusual architectures, which share a macrocyclic peptidyl core that contains a six-membered heterocycle domain central to multiple azoles and dehydroamino acids.[1] To date, over 100 distinct thiopeptides have been identified and are classified into five series *a*—*e* based on the oxidation state of the central, six-membered nitrogenous ring in the core macrocycle (Figure 1A). Despite the diverse and impressive activity of thiopeptides, their general physical drawbacks (*e.g.*, poor water solubility) have largely stymied their clinical use, which has motivated interest in new analog development to overcome these obstacles.[2] However, the complex architecture of thiopeptides and the limited sites for further functionalization pose tremendous challenges to the development of analogs by chemical syntheses and semisyntheses, making researchers turn their attention toward bioengineering and synthetic biology,[3-4] which relies on the elucidation of the biosynthetic pathways of thiopeptides in recent years.[5-7]

As with many RiPPs,[8] the biosynthesis of thiopeptide antibiotics starts with the conversion of a peptide precursor composed of an N-terminal leader sequence and a C-terminal core sequence. A myriad of post-translational modifications (PTMs) occur solely on the latter, in manners either dependent or independent of the former.[9-10] The establishment of the characteristic thiopeptide framework requires Cys/Ser-residue processing to produce azoles,[11] Ser/Thr-residue dehydration to yield dehydroamino acids,[12] and intramolecular cross-bridging to furnish the central heterocyclic domain.[13] Recent studies indicated that the central pyridine heterocycle of series *d* thiopeptides is installed by a cyclase that condenses two dehydroalanine (Dha) residues of a linear precursor in a [4 + 2] cycloaddition, followed by the dehydration and elimination of the leader peptide to generate the aromatic nitrogenous heterocycle.[14] The core macrocycles of series *a* and series *b* thiopeptides also originate from two Dha residues, but it remains poorly understood how this macrocyclization process leads to retention of the N-terminal peptide and a more reduced piperidine or dehydropiperidine ring. Thiopeptins (TPPs, Figure 1B, 1—4) are a complex of thiopeptide antibiotics produced by *Streptomyces tateyamensis* ATCC 21389, possessing either a piperidine or dehydropiperdine in the core macrocycle.[15] The structures of TPPs are similar to the prototypical thiopeptide thiostrepton (TSR, Figure 1B, 5). Both contain 17 amino acids, differing only in the first residue, and both bear a quinaldic acid (QA) moiety within the side-ring system of their core macrocycles, which originates from l-Trp and is formed independently of the precursor peptide through complex ring expansion and recyclization, relying on the activities of the pyridoxal-5'-phosphate-dependent protein TsrA and the flavoprotein TsrE in TSR biosynthesis.[16-17] The conjugation of QA and the N-terminus of the core peptide sequence was also recently confirmed to be catalyzed by an α/β-hydrolase fold protein TsrI during the formation of the side-ring system of TSR.[18] Here, we demonstrate that the central piperidine heterocycle of series *a* thiopeptides is transformed from the dehydropiperidine heterocycle, which relies on the activity of a flexible $F_{420}H_2$-dependent reductase, by exploiting and characterizing the biosynthetic pathway of TPPs, and establishing a series of thiopeptide analogs for clinical drug screening.

Results and Discussion

Identification of the gene(s) responsible for the formation of piperidine in TPPs

To elucidate the biosynthetic mechanism of piperidine in

*E-mail: wliu@sioc.ac.cn, Tel: 86-21-54925111, Fax: 86-21-64166128
‡ These Authors contributed equally to this work.

For submission: https://mc.manuscriptcentral.com/cjoc
For articles: https://onlinelibrary.wiley.com/journal/16147065

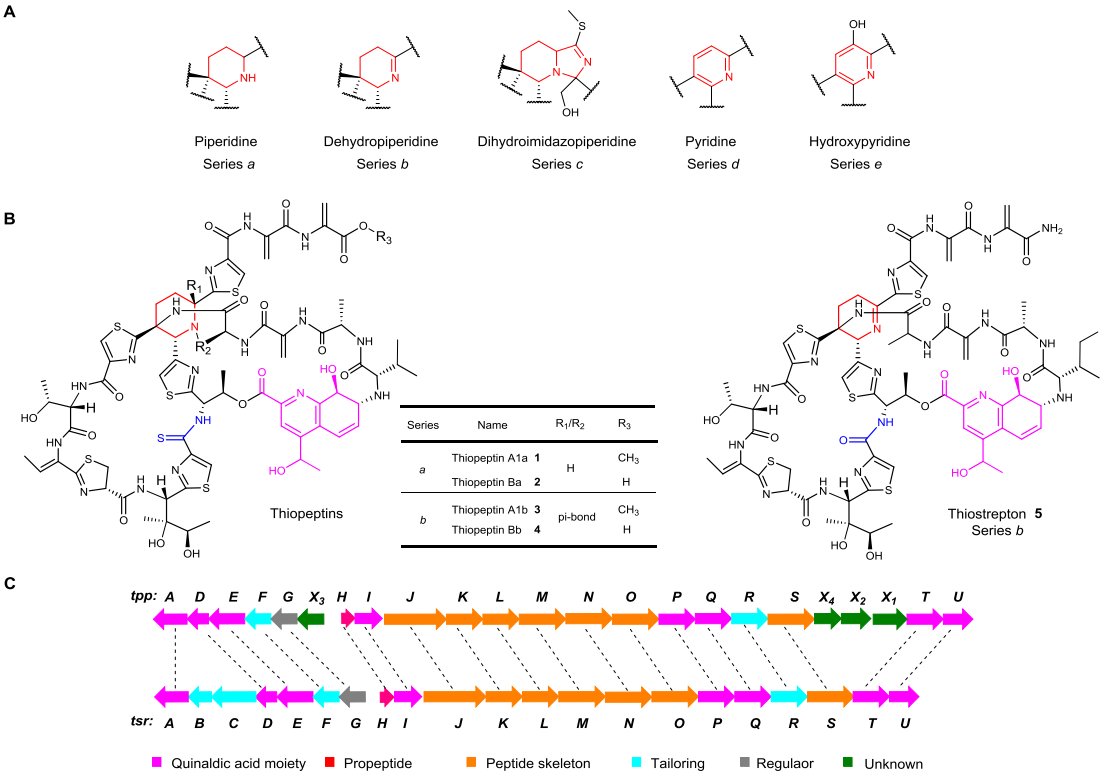

Figure 1 Thiopeptide subfamilies, structures and biosynthetic gene clusters of thiopeptins and thiostrepton. (A) Five subfamilies of thiopeptides series *a*—*e*. (B) Structures of thiopeptins and thiostrepton. The (dehydro)piperidine rings are shown in red, the (thio)amide moiety is shown in blue, and the quinaldic acid moiety is shown in purple red. (C) Biosynthetic gene clusters of thiopeptins and thiostrepton. Homologous genes are indicated by dashed lines.

thiopeptides, we began with the investigation of the gene(s) responsible for the formation of piperidine in TPPs. The TPPs-producing strain *S. tateyamensis* was sequenced and sought for a nucleotide sequence that could encode the core peptide of TPPs (V_1ASASCTTCICTCSCS$_{17}$). *tppH* was then identified as the gene encoding the thiopeptins precursor peptide and the whole sequence of *tpp* was located and named on the basis of being similar in composition and organization to the thiostrepton gene (*tsr*) cluster, which revealed 23 open reading frames (orfs) (Figure 1C and Table S1). By analysis of the sequence homology with *tsr* and other thiopeptide biosynthetic gene clusters, the deduced products of seven orfs, *tppJKLMNOS*, were expected to be required to act on the precursor TppH to afford the core thiopeptins scaffold. TppN and TppO are similar to leader peptide binding proteins and YcaO domain-containing cyclodehydratases, respectively, which are functionally associated with the formation of thiazoline, followed by oxidation by the dehydrogenase TppM to form thiazole.[14,19] The dehydratases TppJ, TppK and TppS are expected to catalyze the dehydrations of Ser/Thr to generate dehydroalanine (Dha)/dehydrobutyrine (Dhb),[14] and then two Dha residues are likely coupled together by a putative [4 + 2] cyclase, TppL, to form a dehydropiperidine and the thiopeptins core macrocycle (Figure S1).

Other *orfs* were presumed to be responsible for the specific post-translational modifications of the core thiopeptins scaffold. The formation of quinoline ketone, a key intermediate for QA moiety, relies on TppTAE, which are similar to the radical SAM and cobalamin-dependent methyltransferase TsrT,[20] the aminotransferase TsrA and the flavin-dependent oxidase TsrE, respectively.[16] TppU, a stereospecific reductase with similarity to TsrU, catalyzes the further conversion of the ketone into an enantiomerically pure *S*-alcohol,[21] while TppPQI were expected to install the QA-containing side ring system.[18,22] According to the previous introduction, the C-termini of thiopeptins from *S. tateyamensis* possess either a methyl ester (**1**, **3**) or a carboxylic acid (**2**, **4**), and thiopeptins containing an amide at the C-termini was not observed. Accordingly, TppF, with similarity to methyltransferase TsrF, may function as a carboxy methyltransferase to produce a C-terminal methyl ester, and a homologue encoding the thiostrepton amidotransferase TsrC is absent.[23] However, there is no homologue of the methylesterase TsrB in the *tpp* cluster, which is responsible for the hydrolysis of the C-terminal methyl ester to produce the carboxylic acid, making it unclear how the C-terminal carboxylic acid of the thiopeptins is formed.

In addition to the different modifications of C-termini between thiopeptins and thiostrepton, TPPs are distinguished by the formation of a thioamide moiety and a piperidine in the core macrocycle. Consistent with the differences in structure, the *tpp* cluster reveals four more genes, *tppX*$_1$/*X*$_2$/*X*$_3$/*X*$_4$ that do not share homology with known thiopeptide biosynthetic genes and may be related to the formation of the thioamide and piperidine. Analysis of the functions of the products encoded by these four genes revealed that TppX$_3$ is similar to an α/β-hydrolase and likely functions as TsrB to hydrolyze the C-terminal methyl ester to produce the carboxylic acid. TppX$_1$/X$_2$ show similarity to TfuA-like proteins and YcaO proteins, respectively. Recent studies showed that such homologous YcaO-TfuA pair is also encoded in the biosynthetic gene cluster of thioviridamide,[24] another thioamide-containing RiPP, and is required for the formation of the post-translational thioamide of methyl-coenzyme A reductase in *Methanosarcina acetivorans*.[25-26] Therefore, it is expected that TppX$_1$ and TppX$_2$ work together to install the thiopeptins thioamide. The only remaining protein encoded by the gene *tppX*$_4$ belongs to pyridoxine 5'-phosphate (PNP) oxidase-like and flavin reductase-like (PNPOx/FlaRed_like) superfamily or PPOX class proteins. The PNPOx/FlaRed_like superfamily proteins are reported as flavin mononu-

cleotide (FMN)-dependent pyridoxine/pyridoxamine 5'-phosphate (PMP) oxidases and other flavin-dependent oxidoreductases (*e.g.*, flavin adenine dinucleotide, FAD),[27-28] while PPOX class are F_{420}-dependent oxidoreductases.[29] Both of these could be candidates to mediate the reduction reaction to form the piperidine ring of series *a* thiopeptins.

Characterization of $TppX_4$ *in vivo*

To clarify the question of whether the piperidine ring of series *a* thiopeptins relies on the activity of $TppX_4$, we inactivated the gene encoding $TppX_4$ in *S. tateyamensis* by in-frame deletion (to exclude the polar effects on downstream gene expression) using a Cas9-contained shuttle plasmid, pWHU2653.[30] The resulting mutant strain Δ*tppX*$_4$ (JY101) completely lost the ability to produce **1** (minor) and **2** (major), which are yielded by wide type *S. tateyamensis* (Figure 2A). However, the mutant produced two distinct compounds **3** (minor) ($[M+Na]^+$ *m/z*: calcd 1703.4394 for $C_{72}H_{84}N_{18}O_{18}NaS_6$, found 1703.4427) and **4** (major) ($[M+H]^+$ *m/z*: calcd 1667.4457 for $C_{71}H_{83}N_{18}O_{18}S_6$, found 1667.4451) with a mass reduced 2 Da relative to **1** and **2**, respectively, and displaying UV-vis absorptions (at λ_{max} = 198, 252, and 305 nm; Figure S2) quite similar to those of the parent compounds **1** and **2**. For structural elucidation, purified **4** was subjected to comparative NMR spectroscopic analysis with **2**. In spite of the overall similarity in the spectra (Figure S7 and Table S5), the distinct signals showed its only difference to be in the central nitrogen heterocycle. The ^{13}C NMR spectrum of compound **4** showed a carbon at δ 163.4, representing a downfield shift of 106.5 from that at δ 56.9 for **2**, while ^1H NMR spectrum showed the correlated hydrogen at δ 4.44 for **2** was absent in **4**. Together with its ^1H-^1H COSY, HSQC, and HMBC spectra, these data established that **4** is a thiopeptin intermediate bearing a dehydropiperidine at the central nitrogen heterocycle (Figure 2A), strongly supporting the conclusion that $TppX_4$ mediates the reduction of dehydropiperidine to form the piperidine ring of series *a* thiopeptins.

$TppX_4$ is an $F_{420}H_2$-dependent dehydropiperidine reductase

Bioinformatics suggests that $TppX_4$ is either a PNPOx/FlaRed_ like protein or a PPOX-class protein, which means that the cofactor of $TppX_4$ could be FMN, FAD or F_{420} (Figure S5). As the $TppX_4$ mediates the hydrogenation of dehydropiperidine, the real cofactor utilized by the enzyme should be the reduced form of those cofactors (*e.g.*, $FMNH_2$, $FADH_2$ or $F_{420}H_2$). To explore the nature of $TppX_4$ catalysis, we overexpressed $TppX_4$ in a 6-His-tagged form and purified it from *Escherichia coli* B12(DE3) (Figure S3). The recombinant $TppX_4$ protein was colorless, suggesting that it did not co-purify with the flavins present in *E. coli*. We then used **4**, isolated from the mutant Δ*tppX*$_4$, as the substrate of $TppX_4$ to reconstitute its activity *in vitro*. First, we tried the reduced flavin as the cofactor of $TppX_4$. Fre,[31] a flavin reductase, was purified from *E. coli* and complemented to the reaction mixture to recycle $FADH_2$/$FMNH_2$ from oxidized FAD/FMN with nicotinamide adenine dinucleotide phosphate (NADPH) *in situ*. However, no matter whether $FADH_2$ or $FMNH_2$ was present in the reaction mixture, it did not result in further transformation of **4** (Figure 2B).

We then considered the cofactor $F_{420}H_2$. Since F_{420} cannot be produced by *E. coli*, we isolated it from an F_{420} high-yield strain, *Mycobacterium smegmatis* mc^2 155.[32] $TppX_5$, an F_{420} reductase, was explored and purified from TPPs-producing strain *S. tateyamensis* (Figure S3) and complemented to the reaction mixture to recycle $F_{420}H_2$ from oxidized F_{420} with NADPH *in situ*. In the presence of $TppX_5$, F_{420} and NADPH, $TppX_4$ completely converted **4** to **2** ($[M+H]^+$ *m/z*: calcd 1669.4613 for $C_{71}H_{85}N_{18}O_{18}S_6$, found 1669.4596) at 30 °C after 5 h, as detected by HPLC and LC-MS (Figure 2B). This transformation failed to occur in the absence of $TppX_5$, F_{420} or NADPH, clearly indicating that $TppX_4$ is a $F_{420}H_2$-dependent dehydropiperidine reductase (Figure 2B). Searching the homologues of $TppX_4$ in NCBI revealed potential piperidine-containing thiopeptide biosynthetic gene clusters and the homologues of $TppX_4$ are present in all reported series *a* thiopeptide biosynthetic gene clusters (Figure S4),[33] demonstrating that it is a common strategy that piperidine of series *a* thiopeptide originates from the reduction of dehydropiperidine of series *b* thiopeptide by an $F_{420}H_2$-dependent reductase. However, it is not yet known if $TppX_4$ would act upon a dehydropiperidine-containing monocyclic intermediate that the second QA-containing macrocycle has not yet installed.

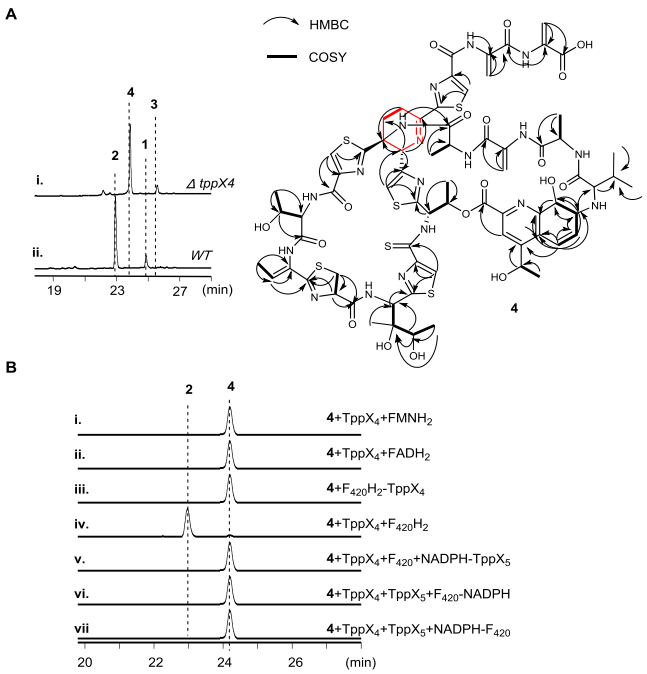

Figure 2 Characterization of the role of $TppX_4$ in the formation of piperidine. (A) *In vivo* assays of $TppX_4$ activity. HPLC analyses of culture extracts from mutant Δ*tppX*$_4$ (i) and wild type *S. tateyamensis* (ii). (B) *In vitro* assays of $TppX_4$ activity. $FADH_2$/$FMNH_2$ was produced by reducing FAD/FMN with NADPH in the presence of Fre. $F_{420}H_2$ was produced by reducing F_{420} with NADPH in the presence of $TppX_5$. i and ii, transforming **4** with cofactor $FADH_2$ and $FMNH_2$, respectively; iii and iv, transforming **4** with cofactor $F_{420}H_2$ in the absence (negative control) and presence of $TppX_4$, respectively; v, transforming **4** in the absence of $TppX_5$; vi, transforming **4** in the absence of NADPH; vii, transforming **4** in the absence of F_{420}.

Substrate scopes of $TppX_4$

To further investigate the substrate tolerance of $TppX_4$, we selected **3**, possessing a methyl ester at the C-termini, and TSR (**5**), a thioamide-free bicyclic thiopeptide containing an amide at the C-termini (Figure1B), as the substrate, respectively. Intriguingly, both of these substrates could be recognized by $TppX_4$ and effectively converted to the corresponding piperidine-containing thiopeptide analogs **1** and **6**, respectively, which were detected by HPLC and LC-MS. The new product **6** was further confirmed by comparative NMR spectra (Figure 3A, Figure S6), indicating that $TppX_4$ is a flexible reductase that can tolerate changes in the C-termini of substrates and thioamide-free bicyclic thiopeptides. To clarify whether $TppX_4$ could act upon a dehydropiperidine-containing monocyclic intermediate, we utilized **7**, which was recently isolated from a mutant strain Δ*tsrP* (Figure 3B), as the substrate.[22] To our delight, $TppX_4$ could effectively catalyze **7** to generate a novel piperidine-containing monocyclic thiopeptide analog **8** ($[M+H]^+$ *m/z*: calcd 1467.3837 for $C_{63}H_{70}N_{16}O_{16}S_5$, found

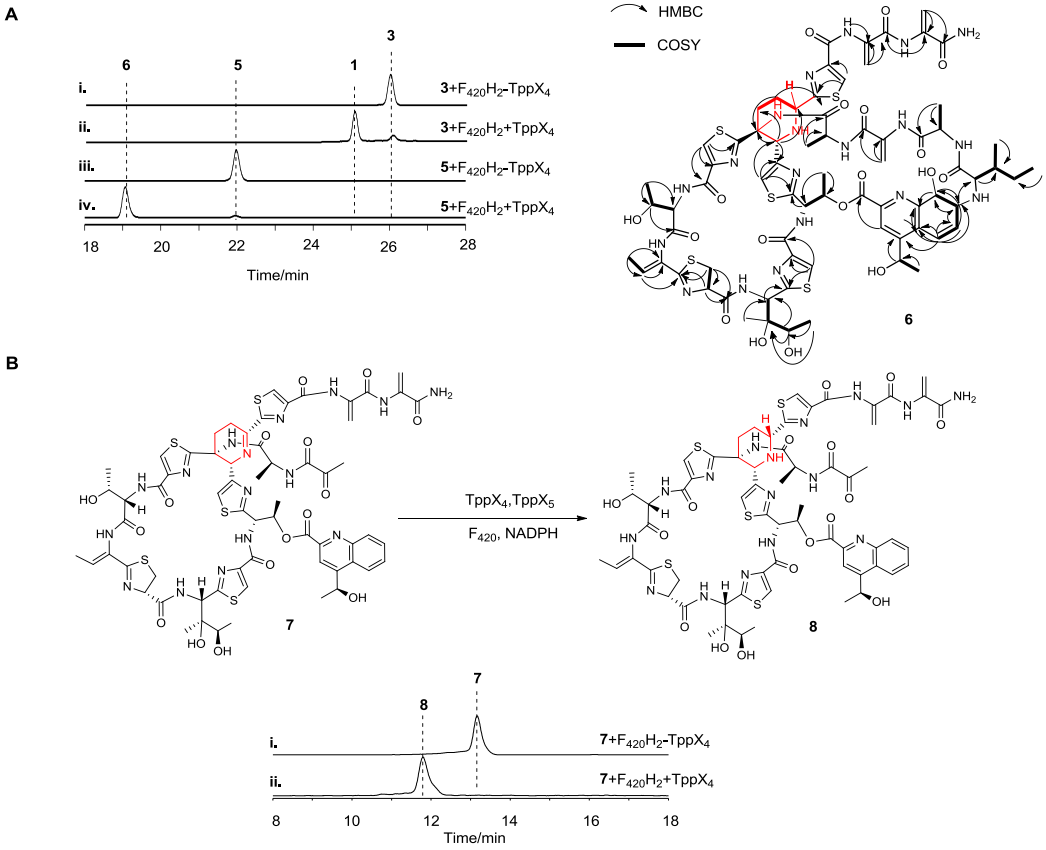

Figure 3 Exploration of the substrate scope of $TppX_4$. (A) *In vitro* transformation of **3** to **1** in the absence (i) and presence (ii) of $TppX_4$; *In vitro* transformation of **5** to **6** in the absence (iii) and presence (iv) of $TppX_4$. (B) $TppX_4$-catalyzed reduction of **7** to **8**, transforming **7** in the absence (i) and presence (ii) of $TppX_4$.

1467.3816), indicating that the formation of piperidine in series *a* thiopeptide can happen before or after the installation of the second QA-containing macrocycle. The results provided here set a solid foundation for the subsequent application of $TppX_4$ to generate a series of piperidine-containing monocyclic or bicyclic thiopeptide analogs for clinical drug screening.

Conclusions

In summary, we demonstrate that the formation of piperidine in thiopeptins relies on an unusual $F_{420}H_2$-dependent reductase $TppX_4$, which can reduce the dehydropiperidine, formed after the [4+2] condensation that assembles the core macrocycle to piperidine. As homologs of $TppX_4$ are present in all available related biosynthetic pathways, the strategy provided here should be common for piperidine-containing thiopeptides (series *a*). Further investigation of the substrate scope of $TppX_4$ shows that it is a flexible reductase that can recognize dehydropiperidine-containing monocyclic or bicyclic thiopeptides and can also tolerate the changes in the C-termini of substrates and thioamide-free bicyclic thiopeptides, which enriches the biosynthetic toolbox for development of additional thiopeptide analogs.

Experimental

Materials, bacterial strains, and plasmids

Biochemicals and media were purchased from Sinopharm Chemical Reagent Co., Ltd. (China), Oxoid Ltd. (U.K.) or Sigma-Aldrich Co. LLC. (USA) unless otherwise stated. Enzymes were purchased from Takara Biotechnology Co. Ltd. (China). Restriction endonucleases were purchased from Thermo Fisher Scientific Co. Ltd. (USA). Chemical reagents were purchased from standard commercial sources. The bacterial strains and plasmids used in this study are listed in Supplementary Table 2.

DNA isolation, manipulation, and sequencing

DNA isolation and manipulation in *E. coli* or actinobacteria were carried out according to standard methods.[34,35] PCR amplifications were carried out on an Applied Biosystems Veriti Thermal Cycler using either Taq DNA polymerase (Vazyme Biotech Co. Ltd, China) for routine genotype verification or Kod DNA polymerase (Takara Biotechnology Co., Ltd.) or PrimeSTAR HS DNA polymerase (Takara Biotechnology Co., Ltd. Japan) for high fidelity amplification. Primer synthesis was performed at Shanghai Sangon Biotech Co. Ltd. (China). DNA sequencing was performed at Shanghai Majorbio Biotech Co. Ltd. (China). Primers used for diagnostic PCR are listed in Supplementary Table 3.

Sequence analysis

Biosynthetic gene clusters (BGCc) were mined from microbial genomes using the AntiSMASH web tool. Open reading frames (ORFs) were identified using the FramePlot 4.0beta program (http://nocardia.nih.go.jp/fp4/). The deduced proteins were compared with other known proteins in the databases using available BLAST methods (http://blast.ncbi.nlm.nih.gov/Blast.cgi).

General chemical analysis

High performance liquid chromatography (HPLC) analysis was carried out on an Agilent 1260 HPLC system (Agilent Technologies Inc., USA) equipped with a DAD detector. Semi-preparative HPLC was performed on an Agilent 1100 system. HPLC electrospray ionization MS (HPLC-ESI-MS) and tandem MS (MS/MS) were per-

formed on a Thermo Fisher LTQ Fleet ESI-MS spectrometer (Thermo Fisher Scientific Inc., USA), and the data were analyzed using Thermo Xcalibur software. ESI-high resolution MS (ESI-HR-MS) analysis was carried out on an instrument consisting of a 1260 HPLC system or a 6538 UHD quadrupole time of flight (QTOF) high resolution mass spectrometry (Agilent Technologies, Santa Clara, USA). NMR data were recorded on an Agilent 500 MHz PremiumCompact+ NMR spectrometer (Agilent Technologies Inc., USA) or on the BrukerDRX400 and Bruker AV500 spectrometers (Bruker Co. Ltd, Germany).

Gene inactivation of $TppX_4$

Genomic DNA of *Streptomyces tateyamensis* ATCC21389 wild-type strain served as the template for PCR amplification unless otherwise stated. To exclude polar effects on downstream gene expression, gene inactivation in *S. tateyamensis* ATCC21389 was performed by in-frame deletion. The gene $tppX_4$ was inactivated using a modified CRISPR-Editing method.[30] Briefly, the 20-bp *sg* sequence was generated and cloned into the plasmid pWHU2653 through homologous recombination among the two 140-bp PCR products amplified from pWHU2653 using the primer pairs sg-for/$tppX_4$-sg-rev and $tppX_4$-sg-for/sg-rev, respectively (Table S3), and *Nhe*I/*Xba*I-digested pWHU2653, yielding pJY1001. 2-kb PCR products amplified from the genome of *Streptomyces tateyamensis* using the primer pairs $tppX_4$-L-for/$tppX_4$-L-rev and $tppX_4$-R-for/$tppX_4$-R-rev were digested by *Eco*RI/*Xba*I and *Xba*I/*Hind*III, respectively (Table S3). A truncated gene, in which a 210 bp in-frame coding region of $tppX_4$ is deleted, was then constructed in *Eco*RI/*Hind*III-digested pKC1139 with these 2-kb PCR products to yield pYJ1002. Ligation of fragments obtained by using *Hind*III to digest pYJ1002 and *Hind*III-digested pJY1001 leads to the production of pJY1003. This recombinant plasmid was then introduced into *S. tateyamensis* by conjugation. The colonies that were apramycin-resistant at 37 °C were identified as integrating mutants, in which a single-crossover homologous recombination event took place. These mutants were cultured for several rounds in the absence of apramycin, and the resulting apramycin-sensitive isolates were subjected to PCR amplification to examine the genotype of the *S. tateyamensis* mutant strain JY101 (Figure S3). PCR amplification for examination primers were $tppX_4$-for/$tppX_4$-rev (Table S3).

Fermentation and isolation of F_{420}

A procedure for purifying F_{420} from cells was developed by using reverse silica gel column (rp-18，25—40 μm, merck, USA) and Semi-preparative separation (SB-C18, 5 μm, 9.4 × 250 mm, Aglient Technologies Inc., USA). Inoculum medium contained 25 g soluble starch, 5 g glucose, 10 g soy peptone, 5 g yeast extract, 2 g ammonium sulfate, and 0.3 g KH_2PO_4 per liter. MSR production medium contained 40 g glucose, 15 g yeast extract, 15 g soy peptone, 1.75 g $NaH_2PO_4{\cdot}H_2O$, and 0.04 g ferric ammonium citrate per liter. MSR medium pH was adjusted to 7.0 before autoclaving. As for the cultivation of the cell, *Mycobacterium smegmatis* mc^2 155 was spread on LB plates and then incubated at 37 °C for 4 d. Approximately 1 cm^2 of the thallus agar of *M. smegmatis* was cut, chopped, and inoculated into inoculum medium. After incubation at 37 °C and 220 r/min for 24 h, a 10% inoculation was made into MSR medium. Further incubation was carried out at 37 °C and 220 r/min for 4 d. Thalli were harvested by centrifugation and were resuspended by 25 mmol/L NaH_2PO_4 buffer (pH=7), autoclaved at 121 °C for 10 min, and centrifuged. This procedure should be repeated three more times, and the pooled supernatant was concentrated by lyophilization, and then loaded on a reversed silica gel column eluting by 95% H_2O (containing 0.1% formic acid) and 5% CH_3CN (0.1% formic acid) mixture. According to HPLC analysis, the fractions containing the target compound were combined and lyophilized. Final purification of the F_{420} was carried out on an Aglient Zorbax column (SB-C18, 5 μm, 9.4 × 250 mm, Aglient Technologies Inc., USA) by gradient elution of solvent A (H_2O + 0.1% formic acid) and solvent B (acetonitrile + 0.1% formic acid) with a flow rate of 3 mL/min over 30 min period as follows: *t* = 0 min, 5% B; *t* = 25 min, 100% B; *t* = 26 min, 5% B; *t* = 30 min, 5% B (UV at 380 nm).

Fermentation, examination and isolation of products

The *S. tateyamensis* wild type strain or its mutant derivative was spread on PS5 agar plates that contained the medium composed of 20 g soluble starch, 5 g pharmamedia, and 20 g agar per liter (pH 7.0), and incubated at 28 °C for sporulation and growth. The sporulated *S. tateyamensis* was inoculated into 30 mL of the solid fermentation medium, which was composed of 40 g soluble starch, 5 g glucose, 5 g soybean meal, 14 g casein , 1 g $CaCO_3$ and 20 g agar per liter. After incubation at 28 °C for 96 h, solid fermentation media were cut, chopped and stored at –80 °C before methanol extraction.

For product examination, 2 mL of each solid fermentation medium was chopped and soaked by 2 mL of methanol for 30 min. After centrifugation to remove the residue, the supernatant was evaporated before redissolution in 200 μL methanol. The methanol sample was subjected to HPLC and HPLC-MS analysis on an Agilent Zorbax column (SB-C18, 4.6 × 250 mm, 5μm, Agilent Technologies Inc., USA) by gradient elution of solvent A (H_2O + 0.1% formic acid) and solvent B (acetonitrile + 0.1% formic acid) with a flow rate of 1 mL/min over a 35 min period as follows: *t* = 0 min, 15% B; *t* = 3 min, 15% B; *t* = 6 min, 40% B; *t* = 12 min, 40% B; *t* = 19 min, 55% B; *t* = 22 min, 85% B; *t* = 28 min, 85% B; *t* = 30 min, 15% B; and *t* = 35 min, 15% B. Related data were analyzed using Thermo Xcalibur software.

For compound **4** isolation, 7 L of the solid fermentation broth was cut, chopped and extracted with 3 L of methanol two times. After filtration and concentration, the extract was loaded onto a silica gel column, which was treated with dichloromethane–methanol (0, 1%, 2%, 3%, 4%, 5%, 6%, 7%, 8%, 9%, 10% and 15% MeOH). After HPLC analyses, the fraction containing compound **4** was combined and concentrated to ~50 mg of dried extract. Further purification by RP-HPLC on an Xselect CSH C18 column (250 × 10 mm, 5 μm, Waters Technology Co., Ltd., USA) by gradient elution of solvent A (H_2O + 0.1% formic acid) and solvent B (acetonitrile + 0.1% formic acid) with a flow rate of 3 mL/min over a 33 min period was as follows: T = 0 min, 15% B; T = 3 min, 15% B; T = 25 min, 85% B; T = 30 min, 15% B; and T = 33 min, 15% B.

For compound **6** isolation, the preparative conversion of **5** to **6** was conducted at 30°C for 5 h in 600 mL of the reaction mixture that contained 1 mM **5**, 50 μM $TppX_4$, 50 μM $TppX_4$, 1 mM F_{420}, DMSO 5%, and 10 mM NADPH in 50 mM Tris-HCl buffer (pH 7.5). After extraction and purification, the resulting product **6** was subjected to HPLC analysis on an Agilent Zorbax column (SB-C18, 4.6×250 mm, 5μm, Agilent Technologies Inc., USA). The extract was further purified by RP-HPLC on an Xselect CSH C18 column (250 × 10 mm, 5μm, Waters Technology Co., Ltd., USA) by gradient elution of solvent A (H_2O + 0.1% formic acid) and solvent B (acetonitrile + 0.1% formic acid) with a flow rate of 3 mL/min over a 33 min period as follows: *t* = 0 min, 15% B; *t* = 3 min, 15% B; *t* = 25 min, 85% B; *t* = 30 min, 15% B; and *t* = 33 min, 15% B.

Protein expression and purification

The genes $tppX_4$ and $tppX_5$ were amplified from the genome of *S. tateyamensis* by PCR using the primer pairs $tppX_4$-P-for/$tppX_4$-P-rev and $tppX_5$-P-for/$tppX_5$-P-rev, respectively (Table S3). While $tppX_4$ was cloned into pET28a(+) for the expression of the recombinant $TppX_4$ protein that is tagged by 6×His at N-terminus, $tppX_5$ was cloned into pET37b(+) for the expression of the recombinant protein $TppX_5$, which is tagged by 6×His at C-terminus. The sequences of $tppX_4$ and $tppX_5$ are listed in Supplementary Table 4. The above plasmid derivatives were introduced into *E. coli*

BL21(DE3), respectively. The culture of each resulting recombinant *E. coli* strain was incubated in Luria-Bertani (LB) medium (5 g yeast extract, 10 g tryptone and 10 g NaCl per liter) containing 50 μg/mL kanamycin at 37 °C and 250 r/min until the cell density reached 0.6—0.8 at OD_{600}. Protein expression was induced by the addition of isopropyl-β-*D*-thiogalactopyranoside (IPTG) to a final concentration of 0.1—1 mmol/L, followed by further incubation for 25—30 h at 25 °C or 16 °C. The cells were harvested by centrifugation at 3000 × g for 20 min, flash-frozen and then stored at –80 °C.

E. coli cells were resuspended in lysis buffer (137 mmol/L NaCl, 2.7 mmol/L KCl, 10 mmol/L Na_2HPO_4, 1.8 mmol/L KH_2PO_4, 10% glycerol and 5 mmol/L imidazole, pH 8.0). After disruption by FB-110X Low Temperature Ultra-Pressure Continuous Flow Cell Disrupter (Shanghai Litu Mechanical Equipment Engineering Co., Ltd, China), soluble fractions were collected by centrifugation. Recombinant proteins that contain a 6×His were purified on a HisTrap HP column (GE Healthcare, USA), which was pre-treated with 10 column volumes (CVs) of lysis buffer followed by 10 CVs of wash buffer (137 mmol/L NaCl, 2.7 mmol/L KCl, 10 mmol/L Na_2HPO_4, 1.8 mmol/L KH_2PO_4, 10% glycerol and 40 mmol/L imidazole, pH 7.4), using elution buffer (137 mmol/L NaCl, 2.7 mmol/L KCl, 10 mmol/L Na_2HPO_4, 1.8 mmol/L KH_2PO_4, 10% glycerol and 250 mmol/L imidazole, pH 7.4). Desired protein fractions were concentrated (to 500 μmol/L—1 mmol/L) using Amicon® Ultra-15 Centrifugal Filter Devices (MILLIPORE, USA) and desalted using a PD-10 Desalting Column (GE Healthcare, USA) according to the manufacturer's protocols, and then quantified in concentration by Bradford assay using bovine serum albumin as the standard. The purity of recombinant proteins was determined by sodium dodecyl sulfate polyacrylamide gel electrophoresis (SDS-PAGE) (Figure S3).

In vitro assays of $TppX_4$ activity

Each conversion was conducted at 30 °C for 5 h in 100 μL reaction mixture that contained 500 μmol/L substrates and 50 μmol/L $TppX_4$, 50 μmol/L $TppX_5$, F_{420} 1 mmol/L , DMSO 5%, 10 mmol/L NADPH along with 50 mmol/L TrisCl (pH 7.5). Conversions were quenched by adding equal volumes of acetonitrile, and after centrifugation, reaction mixtures were subjected to HPLC, HPLC-MS and HR-MS analyses. HPLC was conducted on a reversed-phase Agilent ZORBAX column (SB-C18, 4.6 × 250 mm, 5 μm, Agilent Technologies Inc., USA) by gradient elution of solvent A (H_2O + 0.1% formic acid) and solvent B (acetonitrile + 0.1% formic acid) with a flow rate of 1 mL/min over a 35 min period as follows: *t* = 0 min, 15% B; *t* = 3 min, 15% B; *t* = 6 min, 40% B; *t* = 12 min, 40% B; *t* = 19 min, 55% B; *t* = 22 min, 85% B; *t* = 28 min, 85% B; *t* = 30 min, 15% B; and *t* = 35 min, 15% B. Related data were analyzed using Thermo Xcalibur software and Agilent ChemStation.

Supporting Information

The supporting information for this article is available on the WWW under https://doi.org/10.1002/cjoc.201800497.

Acknowledgement

This work was supported in part by grants from NSFC (31430005, 21750004, 21520102004, 21472231, 21605154, and 21621002), CAS (QYZDJ-SSW-SLH037 and XDB20020200), STCSM (17JC1405100 and 15JC1400400), CPSF (BR0800043), and K. C. Wang Education Foundation.

References

[1] Bagley, M. C.; Dale, J. W.; Merritt, E. A.; Xiong, X. Thiopeptide Antibiotics. *Chem. Rev.* **2005**, *105*, 685–714.

[2] Just-Baringo, X.; Albericio, F.; Alvarez, M. Thiopeptide engineering: a multidisciplinary effort towards future drugs. *Angew. Chem. Int. Ed. Engl.* **2014**, *53*, 6602–6616.

[3] Lin, Z.; He, Q.; Liu, W. Bio-inspired engineering of thiopeptide antibiotics advances the expansion of molecular diversity and utility. *Curr. Opin. Biotechnol.* **2017**, *48*, 210–219.

[4] Chen, M.; Liu, J.; Duan, P.; Li, M.; Liu, W. Biosynthesis and molecular engineering of templated natural products. *Natl. Sci. Rev.* **2017**, *4*, 553–575.

[5] Wieland Brown, L. C.; Acker, M. G.; Clardy, J.; Walsh, C. T.; Fischbach, M. A. Thirteen posttranslational modifications convert a 14-residue peptide into the antibiotic thiocillin. *Proc. Natl. Acad. Sci. U. S. A.* **2009**, *106*, 2549–2553.

[6] Liao, R.; Duan, L.; Lei, C.; Pan, H.; Ding, Y.; Zhang, Q.; Chen, D.; Shen, B.; Yu, Y.; Liu, W. Thiopeptide biosynthesis featuring ribosomally synthesized precursor peptides and conserved posttranslational modifications. *Chem. Biol.* **2009**, *16*, 141–147.

[7] Kelly, W. L.; Pan, L.; Li, C. Thiostrepton Biosynthesis: Prototype for a New Family of Bacteriocins. *J. Am. Chem. Soc.* **2009**, *131*, 4327–4334.

[8] Ortega, M. A.; van der Donk, W. A. New Insights into the Biosynthetic Logic of Ribosomally Synthesized and Post-translationally Modified Peptide Natural Products. *Cell Chem. Biol.* **2016**, *23*, 31–44.

[9] Wang, S.; Zhou, S.; Liu, W. Opportunities and challenges from current investigations into the biosynthetic logic of nosiheptide-represented thiopeptide antibiotics. *Curr. Opin. Chem. Biol.* **2013**, *17*, 626–634.

[10] Walsh, C. T.; Acker, M. G.; Bowers, A. A. Thiazolyl peptide antibiotic biosynthesis: a cascade of post-translational modifications on ribosomal nascent proteins. *J. Biol. Chem.* **2010**, *285*, 27525–27531.

[11] Melby, J. O.; Nard, N. J.; Mitchell, D. A. Thiazole/oxazole-modified microcins: complex natural products from ribosomal templates. *Curr. Opin. Chem. Biol.* **2011**, *15*, 369–378.

[12] Ortega, M. A.; Hao, Y.; Zhang, Q.; Walker, M. C.; van der Donk, W. A.; Nair, S. K. Structure and mechanism of the tRNA-dependent lantibiotic dehydratase NisB. *Nature* **2015**, *517*, 509–512.

[13] Wever, W. J.; Bogart, J. W.; Baccile, J. A.; Chan, A. N.; Schroeder, F. C.; Bowers, A. A. Chemoenzymatic Synthesis of Thiazolyl Peptide Natural Products Featuring an Enzyme-Catalyzed Formal [4 + 2] Cycloaddition. *J. Am. Chem. Soc.* **2015**, *137*, 3494–3497.

[14] Hudson, G. A.; Zhang, Z.; Tietz, J. I.; Mitchell, D. A.; van der Donk, W. A. In Vitro Biosynthesis of the Core Scaffold of the Thiopeptide Thiomuracin. *J. Am. Chem. Soc.* **2015**, *137*, 16012–16015.

[15] Miyairi, N.; Miyoshi, T.; Aoki, H.; Kosaka, M.; Ikushima, H. Thiopeptin, a New Feed Additive Antibiotic: Microbiological and Chemical Studies. *Antimicrob. Agents Chemother.* **1972**, *1*, 192–196.

[16] Lin, Z.; Ji, J.; Zhou, S.; Zhang, F.; Wu, J.; Guo, Y.; Liu, W. Processing 2-Methyl-l-Tryptophan through Tandem Transamination and Selective Oxygenation Initiates Indole Ring Expansion in the Biosynthesis of Thiostrepton. *J. Am. Chem. Soc.* **2017**, *139*, 12105–12108.

[17] Mocek, U.; Zeng, Z.; O'Hagan, D.; Zhou, P.; Fan, L. D. G.; Beale, J. M.; Floss, H. G. Biosynthesis of the modified peptide antibiotic thiostrepton in Streptomyces azureus and Streptomyces laurentii. *J. Am. Chem. Soc.* **1993**, *115*, 7992–8001.

[18] Zheng, Q.; Wang, S.; Duan, P.; Liao, R.; Chen, D.; Liu, W. An α/β-hydrolase fold protein in the biosynthesis of thiostrepton exhibits a dual activity for endopeptidyl hydrolysis and epoxide ring opening/macrocyclization. *Proc. Natl. Acad. Sci. U. S. A.* **2016**, *113*, 14318–14323.

[19] Dunbar, K. L.; Chekan, J. R.; Cox, C. L.; Burkhart, B. J.; Nair, S. K.; Mitchell, D. A. Discovery of a new ATP-binding motif involved in peptidic azoline biosynthesis. *Nat. Chem. Biol.* **2014**, *10*, 823–829.

[20] Benjdia, A.; Pierre, S.; Gherasim, C.; Guillot, A.; Carmona, M.; Amara, P.; Banerjee, R.; Berteau, O. The thiostrepton A tryptophan methyltransferase TsrM catalyses a cob(II)alamin-dependent methyl transfer reaction. *Nat. Commun.* **2015**, *6*, 8377.

[21] Duan, L.; Wang, S.; Liao, R.; Liu, W. Insights into Quinaldic Acid Moiety Formation in Thiostrepton Biosynthesis Facilitating Fluorinated Thiopeptide Generation. *Chem. Biol.* **2012**, *19*, 443–448.

[22] Zheng, Q.; Wang, S.; Liao, R.; Liu, W. Precursor-Directed Mutational Biosynthesis Facilitates the Functional Assignment of Two Cytochromes P450 in Thiostrepton Biosynthesis. *ACS Chem. Biol.* **2016**, *11*, 2673–2678.
[23] Liao, R.; Liu, W. Thiostrepton Maturation Involving a Deesterification−Amidation Way To Process the C-Terminally Methylated Peptide Backbone. *J. Am. Chem. Soc.* **2011**, *133*, 2852–2855.
[24] Izawa, M.; Kawasaki, T.; Hayakawa, Y. Cloning and heterologous expression of the thioviridamide biosynthesis gene cluster from Streptomyces olivoviridis. *Appl. Environ. Microbiol.* **2013**, *79*, 7110–7113.
[25] Nayak, D. D.; Mahanta, N.; Mitchell, D. A. Metcalf, W. W. Post-translational thioamidation of methyl-coenzyme M reductase, a key enzyme in methanogenic and methanotrophic Archaea. *Elife* **2017**, *6*, e29218.
[26] Mahanta, N.; Liu, A.; Dong, S.; Nair, S. K.; Mitchell, D. A. *Proc. Natl. Acad. Sci. U. S. A.* **2018**, *115*, 3030–3035.
[27] di Salvo, M. L.; Safo, M. K.; Musayev, F. N.; Bossa, F.; Schirch, V. Structure and mechanism of Escherichia coli pyridoxine 5'-phosphate oxidase. *Biochim. Biophys. Acta* **2003**, *1647*, 76–82.
[28] di Salvo, M. L.; Contestabile, R.; Safo, M. K. Vitamin B(6) salvage enzymes: mechanism, structure and regulation. *Biochim. Biophys. Acta* **2011**, *1814*, 1597–1608.
[29] Canaan, S.; Sulzenbacher, G.; Roig-Zamboni, V.; Scappuccini-Calvo, L.; Frassinetti, F.; Maurin, D.; Cambillau, C.; Bourne, Y. Crystal structure of the conserved hypothetical protein Rv1155 from Mycobacterium tuberculosis. *FEBS Lett.* **2005**, *579*, 215–221.
[30] Zeng, H.; Wen, S.; Xu, W.; He, Z.; Zhai, G.; Liu, Y.; Deng, Z.; Sun, Y. Highly efficient editing of the actinorhodin polyketide chain length factor gene in Streptomyces coelicolor M145 using CRISPR/Cas9-CodA(sm) combined system. *Appl. Microbiol. Biotechnol.* **2015**, *99*, 10575–10585.
[31] Spyrou, G.; Haggard-Ljungquist, E.; Krook, M.; Jornvall, H.; Nilsson, E.; Reichard, P. Characterization of the flavin reductase gene (fre) of Escherichia coli and construction of a plasmid for overproduction of the enzyme. *J. Bacteriol.* **1991**, *173*, 3673–3679.
[32] Isabelle, D.; Simpson, D. R.; Daniels, L. Large-scale production of coenzyme F420-5,6 by using Mycobacterium smegmatis. *Appl. Environ. Microbiol.* **2002**, *68*, 5750–5755.
[33] Schwalen, C. J.; Hudson, G. A.; Kille, B.; Mitchell, D. A. Bioinformatic Expansion and Discovery of Thiopeptide Antibiotics. *J. Am. Chem. Soc.* **2018**, *140*, 9494–9501.
[34] Green, M. R.; Sambrook, J. *Molecular Cloning*: *a Laboratory Manual*, 4th edn, Cold Spring Harbor Laboratory Press, New York, **2012**.
[35] Keiser, T.; Bibb, M, J.; Buttner, M. J.; Chater, K. F.; Hopwood, D. A. *Practical Streptomyces Genetics*, John Innes Foundation, **2000**.

Manuscript received: October 24, 2018
Manuscript revised: November 18, 2018
Manuscript accepted: November 21, 2018
Accepted manuscript online: November 28, 2018

